

Chapter 6

Pulse durations of pump and probe beams: Cross-correlation measurements

6.1 Introduction

The alignment of the pump and probe beams, both spatially and temporally, is one of the most important factors for success in the time-resolved experiments. This task becomes especially difficult when the probe beam is in the soft x-ray region of the spectrum. Here I describe the method by which we successfully overlapped and obtained time-resolved photoelectron signals between the UV pump and soft x-ray beams when using the dual grating set-up for separation of the harmonics. Temporal pulse widths for the 400 and 266 nm pump beams as well as a number of harmonics are extracted from the cross-correlation measurements.

6.2 800 nm + 400 nm

The first step involves rotating both gratings to 0th order reflection of 800 nm and overlapping the 400 nm pump beam with the 800 nm beam in the interaction region. When the 400 nm pump beam is incident on a sample of Xe gas (I.P.=12.1 eV [45]), it takes a 4 photon process to ionize the $5p_{5/2}$ electron. When the 800 nm beam is introduced, provided the beams are overlapped spatially and temporally, a photoelectron peak at higher energy from a $4 + 1'$ ionization process is observed (4 photons 400 nm + 1 photon 800 nm). By maximizing the photoelectron counts in this peak, the overlap is optimized. This is also useful as an in-situ measurement of the cross-correlation between the 800 and 400 nm pulses. By moving the delay stage in 10 μm steps around the peak of the overlap, a series of points are obtained by calculating the area

under the time-correlated photoelectron peak and plotting it as a function of pump-probe delay. Figure 6.1 is an example of a typical cross-correlation signal between the 400 nm and 800 nm pulses. The Gaussian fit to the data has a FWHM of 116 ± 3 fs. Given the temporal width of the 800 nm pulse of 80 ± 5 fs with the autocorrelator, the temporal width of the 400 nm pulse is calculated to be 84 ± 6 fs, assuming Gaussian pulse profiles.

6.3 800 nm + 266 nm

The specularly reflected 800 nm beam can also be overlapped with the 266 nm pump beam with Kr as a target gas. In this case, it takes four photons of 266 nm to ionize krypton (I.P.=14.1 eV [45]). The three photon process, however, is very close to the ionization threshold, and when the 800 nm and 266 nm beams overlap spatially and temporally, photoelectron signals with electron kinetic energies corresponding to $(3 + 1')$ (3 photons 266 + 1 photon 800 nm), $(3 + 2')$ and $(3 + 3')$ multiphoton processes are observed. Signals from the $(3 + 2')$ and $(3 + 3')$ multiphoton processes only are used to make the cross-correlation trace given in Fig. 6.2. The $(3 + 1')$ multiphoton signal continues out to long times (pump-probe delays from 200 fs to 10 ps have been measured). This results from a Rydberg wavepacket excitation in Kr, where the three photon process (266 nm) excites a population into the high-lying Rydberg states leading up to the 5p ionization threshold. The 800 nm pulse then comes in at a later time and ionizes the evolving wavepacket, creating a long-lived signal. Some experiments were done to probe this wavepacket signal, which are outlined in Appendix 1. The cross-correlation signal between the 800 nm and 266 nm pulses has a FWHM of 157 ± 4 fs, giving a 266 nm pulse width of 135 ± 6 fs. Some broadening of the pulse is expected in the third harmonic generation, simply due to the group velocity spread of the wavelengths in the pulse as it passes through several lenses and harmonic generation crystals.

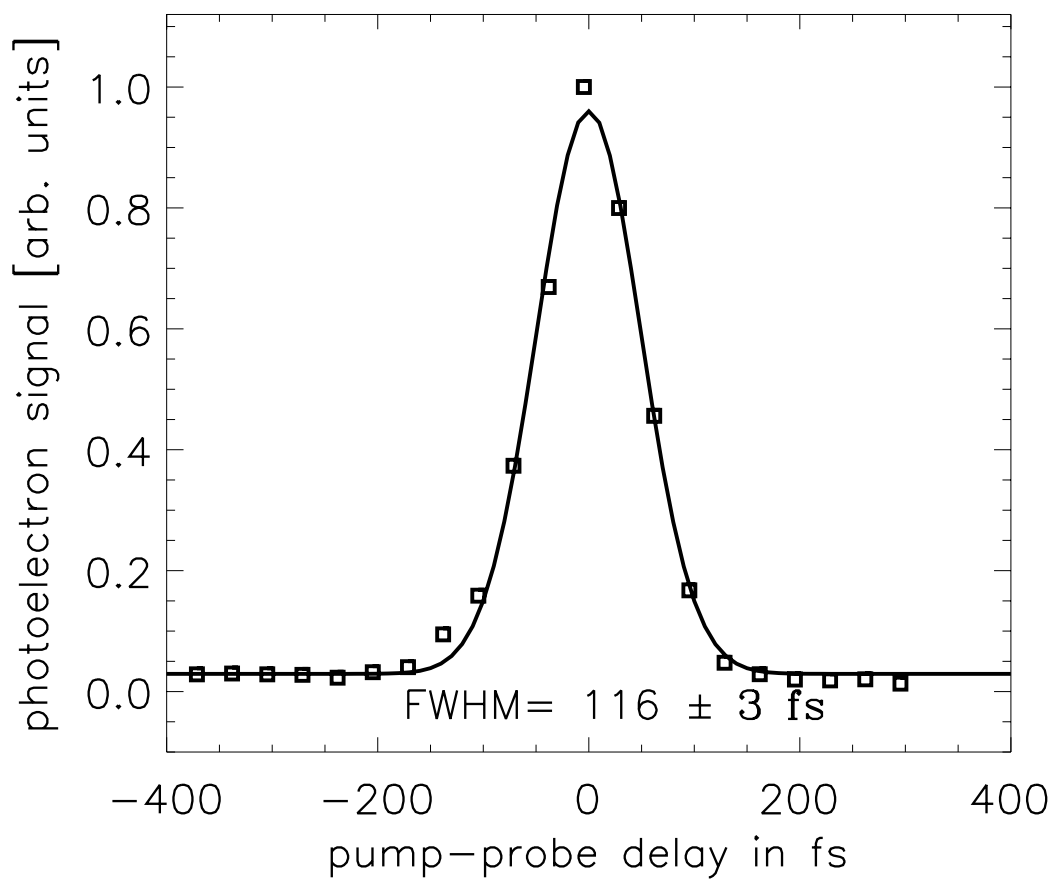


Figure 6.1: A cross-correlation trace of the 800 nm fundamental pulse with the 400 nm pump pulse obtained by a 4 (400 nm photon) + 1' (800 nm photon) multiphoton ionization in Xe.

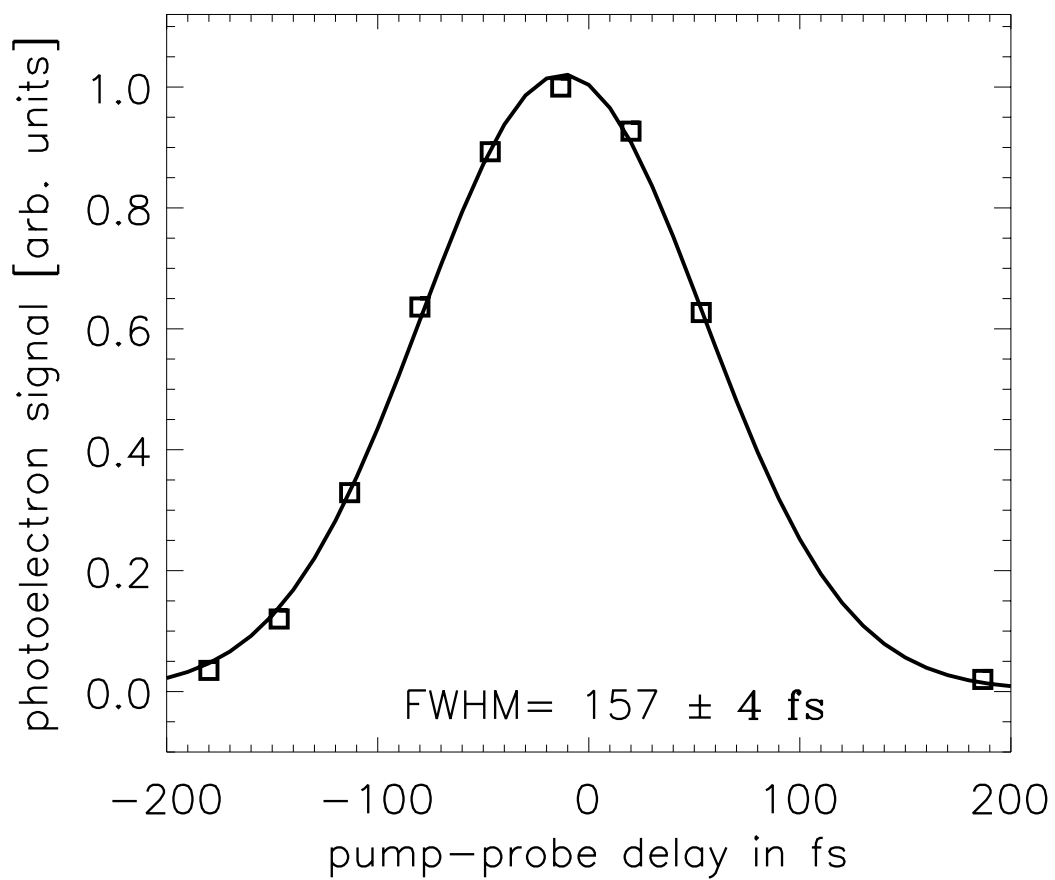


Figure 6.2: A cross-correlation trace of the 800 nm fundamental pulse with the 266 nm pump pulse obtained by a 3 (266 nm photon) + 2' or 3' (800 nm photon) multiphoton ionization in Kr.

6.4 17th harmonic + 800 nm

Once the 800 nm beam is properly aligned, the toroidal grating is rotated to the 17th harmonic, leaving the spherical grating at 0th order. An aperture which is on a translation feedthrough can be moved into the interaction region to ensure that the harmonic beam passes through the same point in space as the 800 nm beam. For the initial attempt at observing a harmonic-visible pump-probe signal, the full 20% of the 800 nm beam that is split off at the beam splitter is used as the pump beam (~ 420 mW average power). With Kr as the sample gas, the 17th harmonic and the 800 nm beam are overlapped in the interaction region. When the pulses overlap at $t=0$, a time correlated signal is observed in the photoelectron spectrum. This signal is an above threshold ionization (ATI) process in which the 17th harmonic first ionizes the Kr sample and the 800 nm pump beam (or dressing beam) adds to or subtracts from the photoelectron energy to create sidebands in the photoelectron spectrum. This ATI process is well documented in the literature [54, 63]. An example of this photoelectron spectrum is shown in Fig. 6.3. With a negative flight tube voltage of ~ 10 V, the main ionization peaks at photoelectron energies of 2.75 and 3.51 eV are seen in both the photoelectron spectra with the 17th harmonic only (solid line) and with the 17th harmonic + 800 nm dressing beam (dashed line). When the dashed line spectrum is expanded, three ATI processes are observed; the addition of one and two 800 nm photons and the subtraction of one 800 nm photon. These peaks increase and decrease as the 17th harmonic pulse and the 800 nm pulse are delayed in time with respect to each other and appear strongest at a delay time of $t = 0$, which is demonstrated in the next section.

6.5 Harmonics + 400 nm

As with the 800 nm beam, cross-correlation signals using Xe as the target gas are observed using the 400 nm pump beam. An example of a photoelectron spectrum with the 17th harmonic and the 400 nm beam overlapped in a sample of Xe is shown in Fig. 6.4(a), while

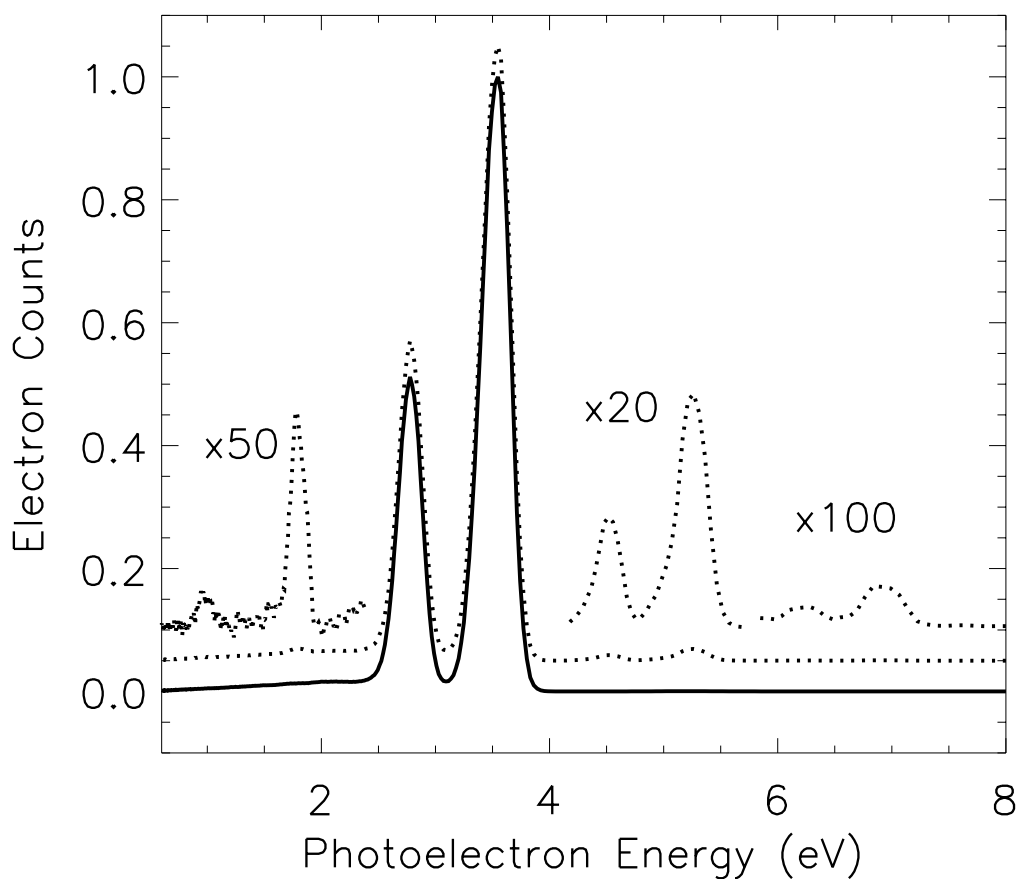


Figure 6.3: Solid line: photoelectron spectrum of Kr gas with the 17th harmonic, showing the spin-orbit split doublet of the Kr^+ ion state. Dashed line: photoelectron spectrum of Kr gas when the 17th harmonic and an 800 nm dressing beam are overlapped spatially and temporally. The 800 nm dressing beam adds to or subtracts from the 17th harmonic ionization in an above threshold ionization process.

Fig. 6.4(b) demonstrates the time-correlation of the sideband peaks as the harmonic pulse is swept across the 400 nm pulse by moving the delay stage. Here we demonstrate that even with a relatively weak 400 nm beam ($\sim 140 \mu\text{J}$ per pulse), we are able to observe the ATI process. In this way, a cross-correlation trace due to the overlap of the 17th harmonic and the 400 nm pulses is obtained in a similar fashion as described above. The cross correlation signal with one grating rotated and the iris before the toroidal grating fully open (8 mm) has a FWHM of 888 ± 100 fs, as is shown in Fig. 6.5(a). When the iris before the toroidal grating is reduced to 1 mm, the cross correlation trace in Fig. 6.5(b) is obtained, which has a FWHM of 441 ± 65 fs. This is an indication that the grating produces a temporal stretching of the harmonic pulse, which we will call pulse front or phase front tilt. The more lines on the grating that are illuminated, the greater the stretching effect on the pulse due to each line delaying the pulse front by one wavelength [34].

There is another common stretching effect induced by using gratings with ultrafast pulses called group velocity dispersion (GVD). This is simply the diffraction-angle spreading by the grating of the range of wavelengths that make up the ultrafast pulse. It is not possible to compensate for both pulse front tilt and GVD stretching effects using two gratings, as the required geometry is different. In a typical stretcher/compressor design in most amplified ultrafast lasers, GVD is compensated by having two gratings effectively facing and parallel to each other so that the path-lengths of the different wavelengths will be equivalent. To compensate for pulse front tilt, the gratings must be in the configuration shown in Fig. 2.6, in order that the part of the beam that reflects from the far end of the first grating (with respect to the source) will be the first to hit the second grating, so that the paths of the different spatial sections of the beam will be equivalent. In this case, since the gratings are used at severe grazing angles, pulse front tilt is the dominant stretching effect.

In our case, the second grating is introduced to compensate for the pulse front tilt stretching effect. Although other frequency selection techniques are available such as deformable mirrors and multi-layer mirrors [29, 64], it is necessary in this experiment to have as clean

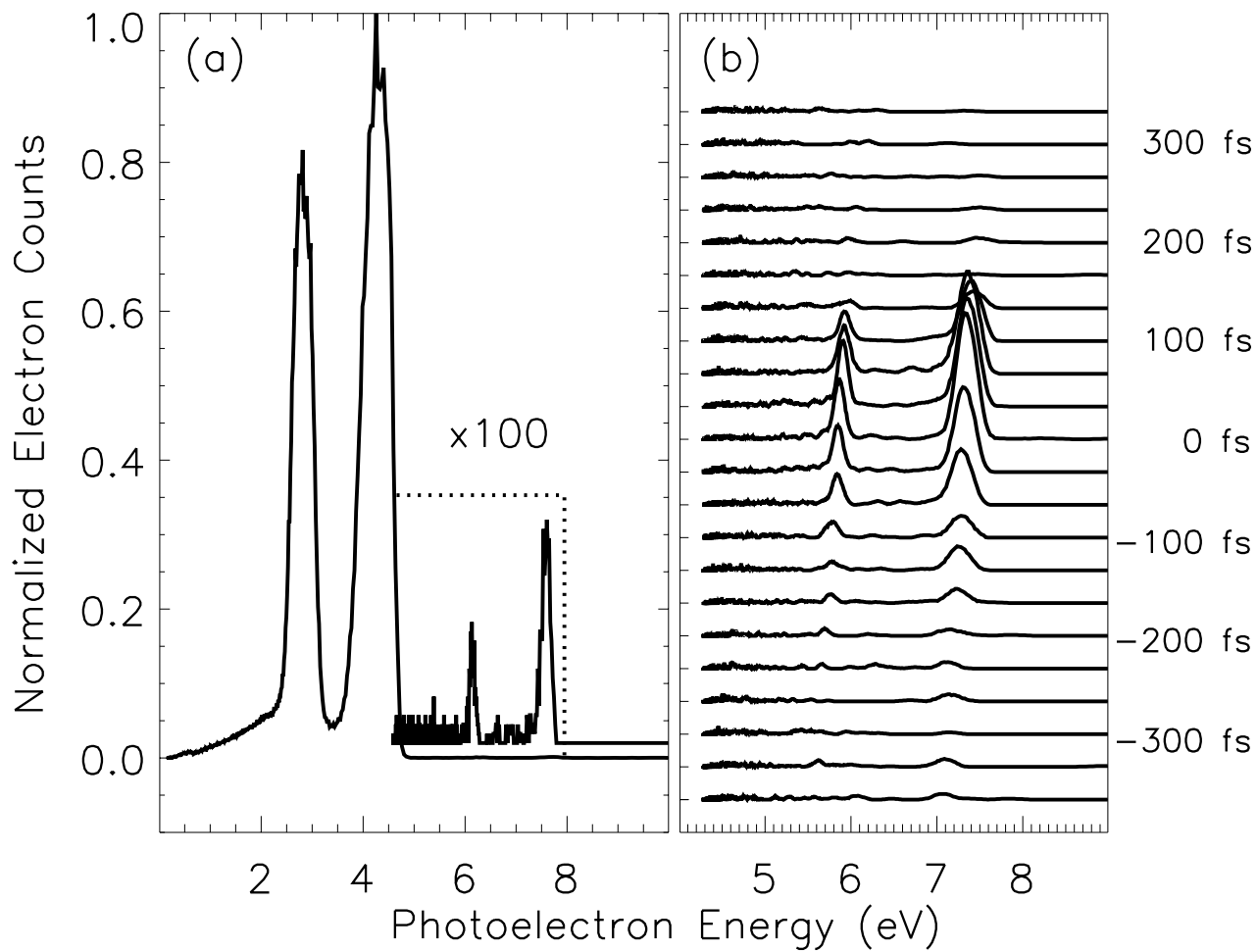


Figure 6.4: (a) A valence level photoelectron spectrum of Xe with the 17th harmonic showing the sidebands created by introduction of the 400 nm dressing pulse with spatial and temporal overlap. The sideband photoelectron peaks are exactly one 400 nm photon higher in energy than the main ionization peaks. (b) The time-correlation of the sideband photoelectron peaks.

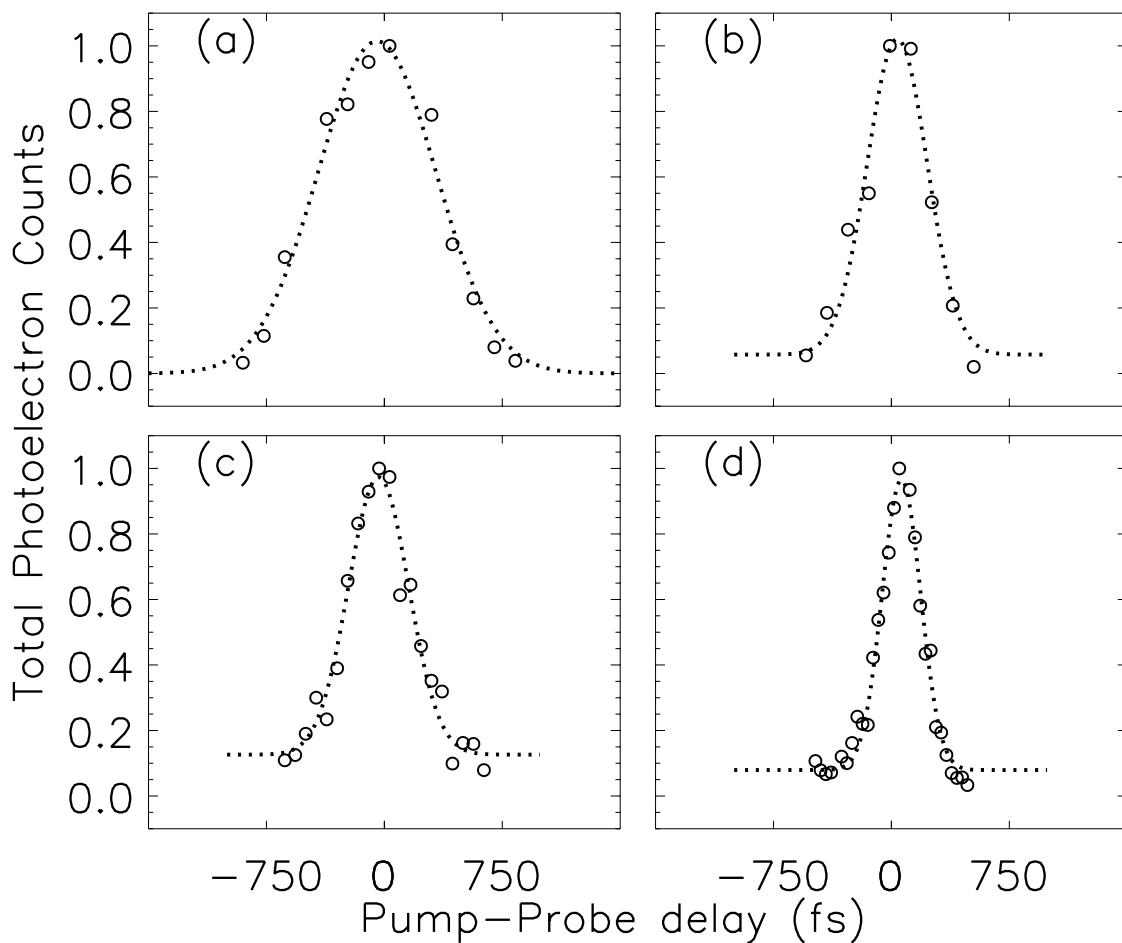


Figure 6.5: Cross-correlation traces of the 17th harmonic + 400 nm in Xe. (a) Toroidal grating rotated to 1st order diffraction, concave grating at 0th order reflection, iris open (8mm), FWHM = 882 ± 105 fs; (b) as (a) except iris at 1 mm, FWHM = 449 ± 64 fs; (c) Both toroidal and concave gratings rotated to 1st order diffraction, iris open (8mm), FWHM = 440 ± 25 fs; (d) as (c) with iris at 1mm, FWHM = 288 ± 12 fs.

a separation of the desired harmonic as possible. This is because pump-probe signatures are small signals (often $\leq 1\%$) above the background signal arising from ground state absorption and ionization of the harmonic. Even a small leakage of neighboring harmonics could mask the desired pump-probe signals. In addition, using gratings allows for a large range of accessible energies with relative ease of switching between harmonics.

When the spherical grating is rotated to 1st order diffraction and the iris before the second grating is 8 mm in diameter, a cross correlation between the 17th and 400 nm beams with a FWHM of 451 ± 32 fs (Fig. 6.5(c)). Comparing this to the width with one grating rotated, an improvement of a factor of 2 in the width of the cross correlation is observed. Again, when reducing the iris to 1 mm, the cross correlation narrows as is shown in Fig. 6.5(d). Although some amount of linear chirp from the gratings is still present, there is still an improvement, with a FWHM of 288 ± 12 fs. Using 84 ± 6 fs as the temporal width of the 400 nm pulse, the shortest 17th harmonic pulse width is calculated to be 275 ± 13 fs.

A ray tracing program was used to find the optimal distance between the two gratings for compression of the harmonic pulse. The distances from the ray tracing optimization are 18.2 cm from the focus in the jet to the center of the spherical grating, 80 cm from the center of the spherical grating to the center of the toroidal grating, and 93.1 cm from the center of the toroidal grating to the slit. The physical dimensions of the system were matched to these numbers with an accuracy of within 1 cm. According to the calculations, the compression would be best for the 21st harmonic for the current chamber dimensions. The distance between the two gratings as well as the number of lines illuminated on the gratings by the harmonic beam are critical parameters in the calculation of the compression. Experimentally, however, it was found that the 19th harmonic has the shortest pulse width. Figure 6.6 demonstrates the shortest soft x-ray pulse achieved to date with this apparatus, with a FWHM of 200 ± 13 fs. Again, using the 84 fs pulse width of the 400 nm pulse, the FWHM of the soft x-ray pulse is calculated to be 182 ± 14 fs. The widths of the neighboring harmonics become wider on either side of the 19th harmonic, with the 21st having a similar width as the 17th harmonic. The temporal widths of all the

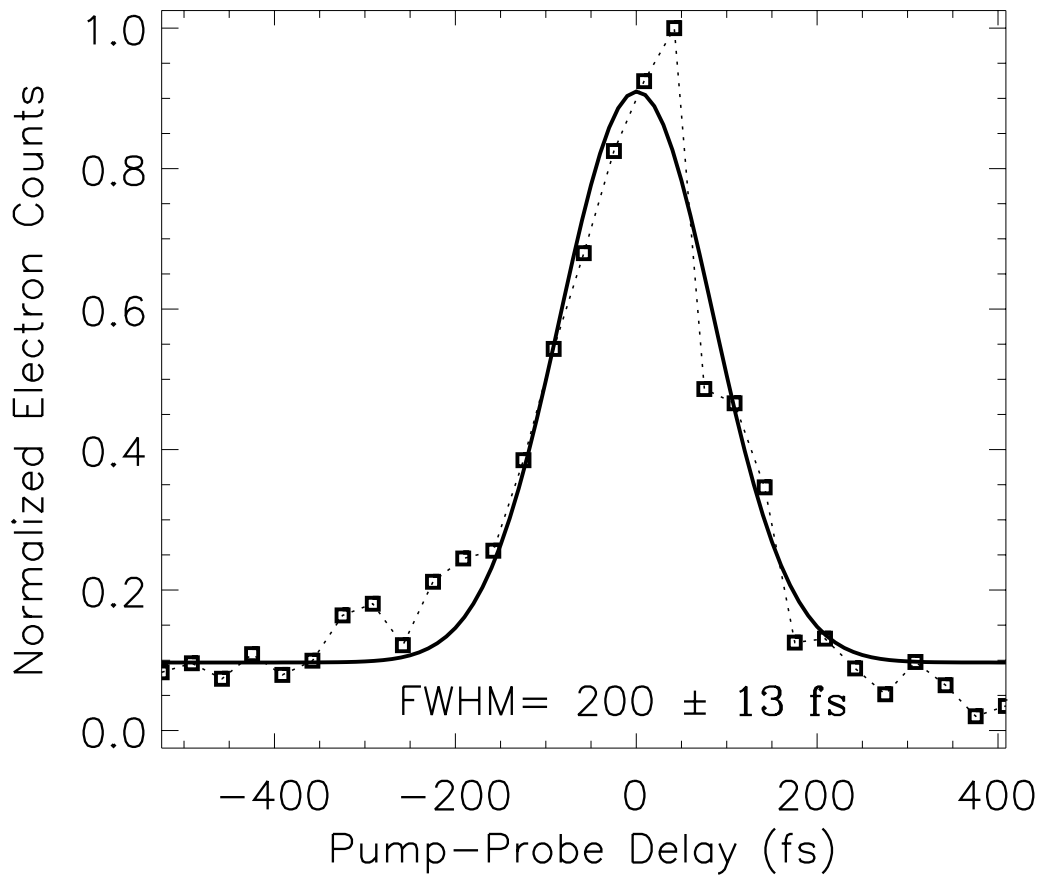


Figure 6.6: Cross-correlation trace of the 19th harmonic + 400 nm in Xe. The shortest soft x-ray pulse measured to date with the instrument described here. Some irregularity in the temporal profile may indicate an irregular spectral profile of the harmonic pulse.

harmonics measured are summarized in Fig. 6.7. It is important to note that the stretching effect of pulse front tilt goes as a function of λ^3 , therefore the higher harmonics (~ 41 st and above) are not expected to suffer from such a large temporal stretching effect, and only the toroidal grating should be required when using the higher harmonics for pump-probe experiments.

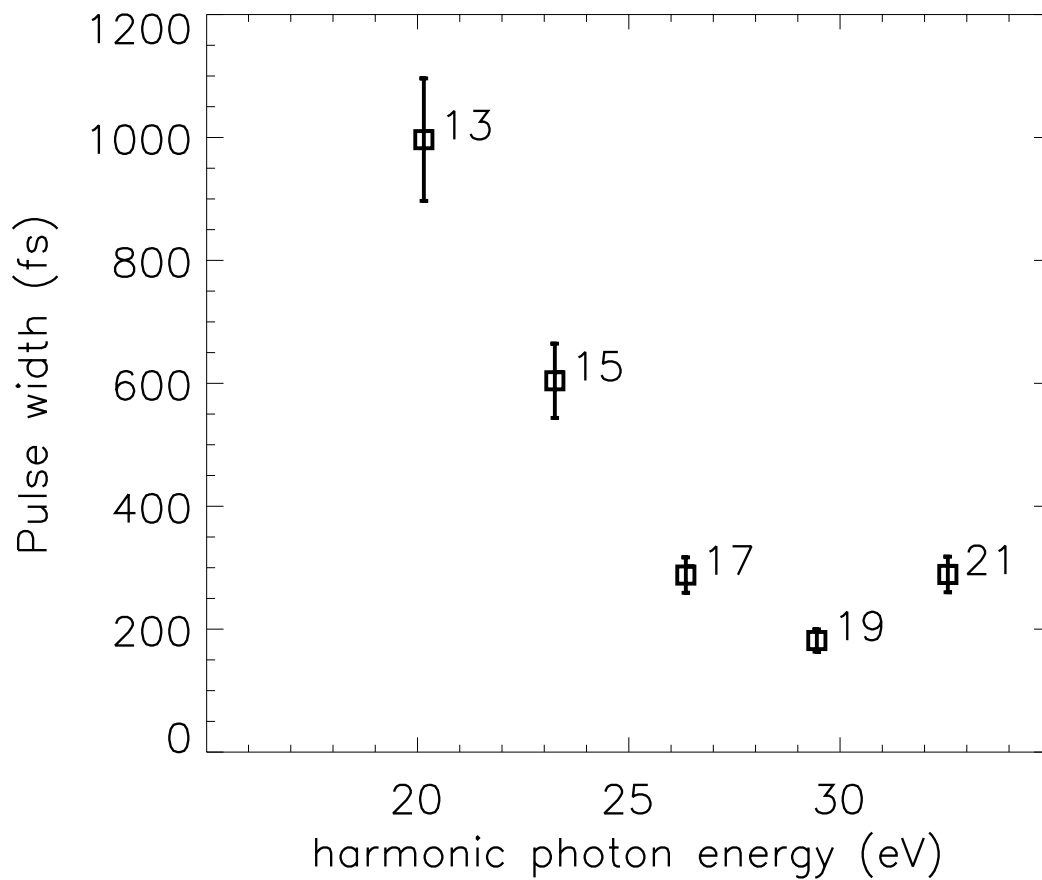


Figure 6.7: The pulse widths of the 13th through the 21st harmonics measured by cross-correlation with a 400 nm pulse. Error bars designate the error in the pulse width given by the Gaussian fitting program.